

Synoptic studies of seventeen blazars detected in very-high-energy gamma rays

R. M. Wagner^{*}

Max-Planck-Institut für Physik, Föhringer Ring 6, D-80805 München, Germany

Submitted to MNRAS 2007 September 13

ABSTRACT

Since 2002, the number of detected blazars at gamma-ray energies above 100 GeV has far more than doubled. I study 17 blazars currently known to emit $E > 100$ GeV gamma rays. Their intrinsic energy spectra are reconstructed by removing extragalactic background light attenuation effects. Luminosity and spectral slope in the $E > 100$ GeV region are then compared and correlated among each other, with X-ray, optical, and radio data, and with the estimated black hole masses of the respective host galaxies. In addition, I consider temporal properties of the X-ray and $E > 100$ GeV gamma-ray flux. Key findings of the studies are correlations between the gamma-ray luminosity and the X-ray luminosity, the synchrotron peak location, and the spectral slope in the $E > 100$ GeV region. No correlations of the gamma emission properties with the central black hole masses are found. As a specific application, the study allows to constrain the still undetermined redshift of the blazar PG 1553+113.

Key words: galaxies: active – BL Lacertae objects: individual (1ES 0229+200, 1ES 0347-121, 1ES 1011+496, 1ES 1101-232, 1ES 1218+304, 1ES 1959+650, 1ES 2344+514, 3C 279, BL Lacertae, H 1426+428, H 2356-309, Mkn 180, Mkn 421, Mkn 501, PG 1553+113, PKS 0548-322, PKS 2005-489, PKS 2155-304).

1 INTRODUCTION

All but one of the detected extragalactic very high energy (VHE, defined by $E > 100$ GeV) gamma (γ) ray sources so far are blazars. Within the unified scheme (e.g., Urry & Padovani 1995) of active galactic nuclei (AGN), blazars comprise the rare and extreme subclasses of BL Lac objects and flat spectrum radio quasars (FSRQs). These are characterised by high apparent luminosities, short variability time scales, and apparent superluminal motion of jet components. These observations can be explained by highly relativistic, beamed plasma outflows (‘jets’) closely aligned to the observer’s line of sight (Blandford & Königl 1979) powered by central supermassive black holes accreting at sub-Eddington rates (Lynden-Bell 1969; Rees 1978). The prime scientific interest in VHE γ -ray emitting blazars (in the following, ‘VHE blazars’) is twofold: (1) To understand the particle acceleration and γ -ray production mechanisms, assumed to take place in the jets and to be linked to the central supermassive massive black hole (BH). Knowledge of the VHE emission process will also contribute to the further understanding of the accretion processes in AGNs, jet formation processes, and the jet structure. (2) To use the VHE γ -rays as a probe of the extragalactic background light (EBL; e.g. Hauser & Dwek 2001; Kashlinsky 2005) spectrum in the wavelength range between about 0.3 to 30 μm . Determining the EBL spectrum in this wavelength range may allow to constrain the star formation rate (convolved

with the initial mass function) in the early Universe. In order to assess both issues, it is essential to have a large sample of VHE γ -ray blazars at hand. Ideally it should encompass a wide range in redshift for EBL studies and at the same time include groups of sources at similar distances in order to probe and compare properties of the individual sources without possible systematic uncertainties caused by the EBL de-absorption.

The preconditions for such studies have much improved recently: Before 2004, only a few nearby extragalactic sources had been established as VHE γ -ray emitters (e.g., Mori 2003) and provided hardly enough data to perform comparative studies. Around 2004, the third generation of imaging air Cerenkov telescopes (IACT, e.g. MAGIC, Baixeras et al. 2004; Cortina et al. 2005 and H.E.S.S., Hinton 2004), the most successful tools so far to explore VHE γ -rays, started to deliver scientific results. To date, the VHE blazar sample comprises 17 objects, among them one LBL object, BL Lacertae. Furthermore, now the redshifts of the known VHE blazars reach up to $z = 0.212$ (or even to $z = 0.536$, considering the recently announced discovery of the first FSRQ in VHE γ -rays, 3C 279, Teshima et al. 2007). M87, a FR I radio galaxy also detected in VHE γ -rays, is not included in this study, as its VHE γ -ray production mechanism may differ from that in blazars (Aharonian et al. 2006c). Fig. 1 shows the sky positions of the known VHE blazars in galactic coordinates along with the AGNs identified in the 3rd EGRET catalogue.

The electromagnetic continuum spectra of blazars extend over many orders of magnitude from radio frequencies to sometimes

^{*} E-mail: robert.wagner@mpp.mpg.de

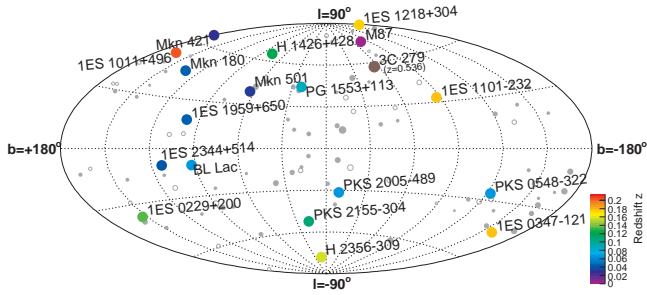


Figure 1. Currently known VHE γ -ray blazars along with the identified (66 objects) and tentatively identified AGNs (27 objects) in the 3rd EGRET catalogue of γ -ray sources (solid grey dots: identified AGNs; open grey dots: tentatively identified AGNs) EGRET data from Hartman et al. (1999). The sources are shown in a galactic coordinate system.

multi-TeV energies and are dominated by non-thermal emission that consists in a νF_ν representation of two pronounced peaks. The low energy peak, located between the IR and hard X-rays, is thought to arise from synchrotron emission of ultrarelativistic electrons, accelerated by shocks moving along the jets at relativistic bulk speed. Depending on the location of the low energy peak, BL Lac objects are often referred to as high-frequency peaked (HBL; in the UV to X-ray domain) or low-frequency peaked (LBL; in the near-IR to optical) BL Lac objects (Fossati et al. 1998), although the transition is smooth rather than dichotomic. The origin of the high-energy peak at MeV to TeV energies is still debated. It is commonly explained by inverse Compton up-scattering of low energy photons by electrons. The seed photons may originate from synchrotron radiation produced by the same electron population (synchrotron-self Compton (SSC) models; e.g. Maraschi, Ghisellini & Celotti 1992; Coppi 1992) or belong to ambient thermal photon fields (external inverse Compton models; e.g. Sikora, Begelman & Rees 1994; Dermer & Schlickeiser 1994). In hadronic models, which can also explain the observed features, interactions of a highly relativistic jet outflow with ambient matter (Dar & Laor 1997; Bednarek 1993), proton-induced cascades (Mannheim 1993), synchrotron radiation by protons (Aharonian 2000; Mücke & Protheroe 2001), or curvature radiation, are responsible for the high energy photons. The AGNs identified in the EGRET data are predominantly powerful FSRQs and quasars with SEDs peaking at rather low frequencies, and thus only few of these (Mkn 421, PKS 2155-304, BL Lacertae, and 3C 279) were also detected in the VHE range.

Knowing the variability time-scales of the VHE γ -ray emission and the form of the two-bump spectral energy distribution (SED) enables the derivation of all input parameters of one-zone SSC models (Tavecchio et al. 1998), which describe the observed emission in BL Lac objects reasonably well. Strictly simultaneous and temporally-resolved measurements of the SED, however, are only rarely possible and more often than not are also severely constrained by the (temporal) instrumental resolution. Generally, detailed spectral studies in particular in low emission states are rather demanding. In addition, the determination of the location of the high-energy peak $\nu_{\text{peak}}^{\text{IC}}$ generally would require complementary satellite detector coverage of the SED between some hundred MeV and ≈ 50 GeV. This region of the SED, however, is difficult to access due to the low fluxes expected (up to ≈ 100 MeV) from extragalactic sources in between the two bumps and due to insufficient instrumental sensitivity for energies exceeding some GeVs.

In this paper, for the first time studies of the VHE emission

Table 1. Extragalactic VHE γ -ray sources, listed in chronological order of their discovery.

Source	Type	Redshift z	Discovery reference
Mkn 421	HBL	0.030	Punch et al. (1992)
Mkn 501	HBL	0.034	Quinn et al. (1996)
1ES 2344+514	HBL	0.044	Catanese et al. (1998)
1ES 1959+650	HBL	0.047	Nishiyama et al. (1999)
PKS 2155-304	HBL	0.116	Chadwick et al. (1999)
H 1426+428	HBL	0.129	Horan et al. (2002)
M87 ^a	FR I	0.0044	Aharonian et al. (2004)
PKS 2005-489	HBL	0.071	Aharonian et al. (2005b)
1ES 1218+304	HBL	0.182	Albert et al. (2006b)
H 2356-309	HBL	0.165	Aharonian et al. (2006a)
1ES 1101-232	HBL	0.186	Aharonian et al. (2006a)
PG 1553+113	HBL	^b	Aharonian et al. (2006b), Albert et al. (2007a)
Mkn 180	HBL	0.045	Albert et al. (2006c)
PKS 0548-322	HBL	0.069	Superina et al. (2007)
BL Lacertae	LBL	0.069	Albert et al. (2007d)
1ES 1011+496	HBL	0.212	Albert et al. (2007e)
1ES 0229+200	HBL	0.139	Raue et al. (2007)
1ES 0347-121	HBL	0.188	Aharonian et al. (2007c)
3C 279 ^c	FSRQ	0.536	Teshima et al. (2007)

The upper part of the table shows the confirmed sources prior to the advent of new generation instruments like MAGIC and H.E.S.S., while the lower panel summarises the sources discovered after 2002. HBL: High-frequency peaked BL Lac object, LBL: Low-frequency peaked BL Lac object, FSRQ: Flat spectrum radio quasar, FR: Fanaroff–Riley galaxy. ^a M87 is not included in the present study. ^b This redshift is currently under discussion, cf. Sect. 5.6. ^c No spectrum of 3C 279 has been published yet.

properties of the complete set of all currently known VHE blazars (cf. Tab. 1) are performed. First, the detected VHE blazars are brought into context with the AGN searches conducted by IACTs so far and the expected γ -ray attenuation by the EBL in Sect. 2. After a study of the black hole mass distribution of the VHE blazars in Sect. 3, we infer intrinsic emission properties in the VHE γ -ray regime in Sect. 4. Because measurements of the location and shape of the high-energy bump are elusive at present for almost all VHE blazars, the observed γ -ray luminosity and spectral slope in the VHE region are used as auxiliary observables to characterise the VHE γ -ray emission. The main part of the paper (Sect. 5.1 to 5.5) is devoted to the search for correlations of these observables with the X-ray emission properties, the optical, and the radio luminosity, and with the black hole mass estimations. In Sect. 5.6 the VHE blazar luminosity distribution is used to address the specific problem of the unknown redshift of PG 1553+113 by deriving an upper redshift for this VHE blazar. Finally, Sect. 5.7 turns to the study of X-ray and VHE γ -ray timing properties. Sect. 6 summarises the main conclusions of the studies.

2 POPULATION STUDIES AND THE γ -RAY HORIZON

When travelling cosmological distances, VHE γ -rays interact with the low energy photons of the EBL (see, e.g. Nikishov 1962; Gould & Schröder 1966; Hauser & Dwek 2001; Kashlinsky 2005). The predominant reaction $\gamma_{\text{VHE}} + \gamma_{\text{EBL}} \rightarrow e^+ e^-$ modifies source-intrinsic γ -ray energy spectra. The cross-section of this process peaks strongly at $E_{\text{CM}} = 1.8 \times (2m_e c^2)$, therefore a given VHE photon energy probes a narrow range of the EBL spectrum. The part of the EBL to which VHE γ -rays are sensitive comprises the

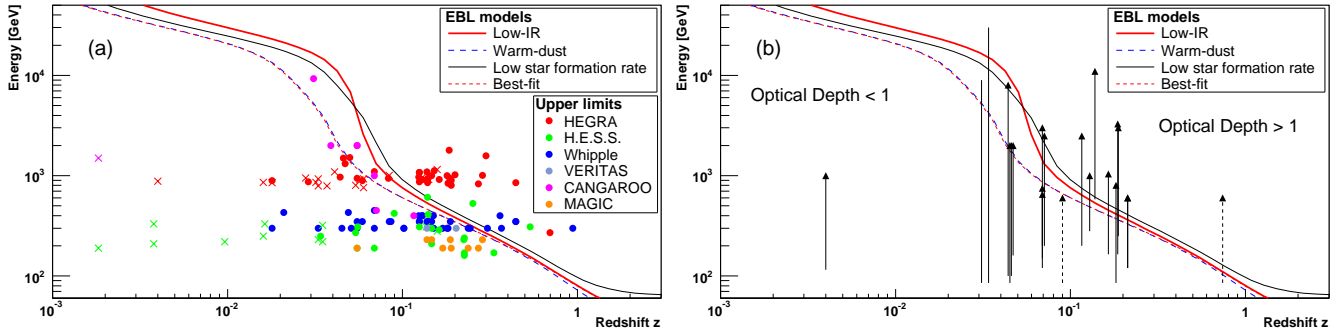


Figure 2. (a) Low energy thresholds from searches for VHE γ -ray emission from AGNs. Dots: blazars, crosses: other AGN types (starburst galaxies, radio galaxies, etc.). The curves represent Fazio–Stecker relations (flux attenuation by a factor e^{-1}) for different EBL models given by Kneiske et al. (2004). Data from searches by HEGRA (Aharonian et al. 2004), H.E.S.S. (Aharonian et al. 2005c; Benbow & Bühler 2007), Whipple (Kerrick et al. 1995; Horan et al. 2004), VERITAS (Cogan 2007), CANGAROO (Nishijima 2002), and MAGIC (Albert et al. 2007g). (b) Detected VHE γ -ray sources (see Tab. 3 for references). Shown are the energy ranges of the measured γ -ray spectra; high-energy cutoffs were found only for Mkn 421 and Mkn 501, for all other sources arrows represent possibly continuing spectra to higher energies. The dashed lines represent PG 1553+113 at the lower and upper limit for its redshift, $z > 0.09$ (Sbarufatti et al. 2006) and $z < 0.74$ (Aharonian et al. 2006b; Albert et al. 2007a).

(redshifted) relic emission of galaxies and star-forming systems and the light absorbed and re-emitted by dust. The EBL attenuation results in a maximum distance over which photons with a particular energy can survive: The Fazio–Stecker relation (FSR) describes the distance at which the optical depth for a VHE photon of a given energy reaches unity (attenuation by a factor e^{-1}). Thus the FSR defines the *cosmological γ -ray horizon*. Fig. 2a shows the instrumental low energy thresholds from searches for VHE γ -ray emission from AGNs. Along with these, the FSR for different EBL models as given by Kneiske et al. (2004) is plotted. The models differ in the IR density, dust properties and the star formation rate in the early Universe. The FSR divides the plot into a region from which no γ -rays can reach the Earth and into another region, in which positive detections are to be expected or a too weak source-intrinsic emission made detections fail (due to insufficient instrumental sensitivity). Obviously, with a decreasing instrumental energy threshold, the visible Universe ‘opens up’, providing access to a larger source population. Current EBL models result in a steepening of the intrinsic spectra from ≈ 200 GeV on (power law spectra are softened, but their shape is approximately retained), while for lower energies the effects are minimal. When an optical depth of one is reached, a quasi-exponential cutoff in the observed spectra occurs. Fig. 2b shows the energy ranges over which blazars in VHE γ radiation have been detected. Up to now, only for the strong, close-by blazars Mkn 421 and Mkn 501 indications of the expected exponential high energy cutoff have been observed thanks to high γ statistics (Aharonian et al. 2001a; Krennrich et al. 2001; Albert et al. 2007c). The observed spectra of all other blazars can be accurately described by power-laws or broken power-laws. While most of the nearby VHE blazars cannot constrain the current EBL models, some of the sources at $z > 0.1$ start challenging these (Aharonian et al. 2006a, 2007c; Teshima et al. 2007), as no cutoffs have been observed so far at the high-energy ends of their γ -ray spectra.

3 BLACK HOLE MASSES IN BLAZARS

It is well established that all galaxies with a massive bulge component host supermassive black holes in their centres (Richstone et al. 1998; Bender & Kormendy 2003). There are a couple of indirect methods to infer the masses of the central BHs: One is to estimate M_{\bullet} using the correlation between M_{\bullet} and the velocity dispersion

σ of the host galaxy ($M - \sigma$ relation, Ferrarese & Merritt 2000; Gebhardt et al. 2000) found from stellar and gas kinematics and maser emission. We estimated the black hole masses of VHE γ -ray emitting blazars using the $M - \sigma$ relation given by Tremaine et al. (2002). This approach assumes that AGN host galaxies are similar to non-active galaxies. The velocity dispersions were collected from the literature or are inferred from the fundamental plane (Djorgovski & Davis 1987), a relation between the central velocity dispersion σ , the effective galaxy radius R_e , and the corresponding surface brightness $\langle \mu_e \rangle$, which is valid for elliptical galaxies, in particular also for AGNs and radio galaxies (Bettoni et al. 2001). Whenever more than one σ value is given in the literature, individual masses were derived for each of the σ values and averaged. The σ values and the resulting black hole masses for the VHE γ -ray blazars studied here are given in Tab. 2.

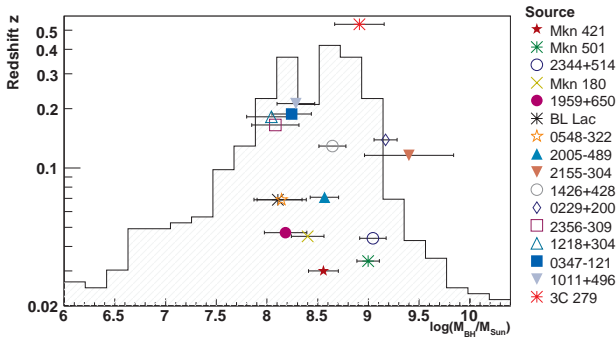
The determination of M_{\bullet} suffers from rather large systematic uncertainties due to the different methods used to derive σ . The relation between M_{\bullet} and bulge luminosity L_B (Kormendy & Richstone 1995) has generally a larger scatter than the $M - \sigma$ relation and was therefore only used for PKS 2155-304, because for this blazar no σ or $\langle \mu_e \rangle$ measurement is available. We used the R -band luminosity given by Falomo (1996) to calculate $\log(M_{\bullet}/M_{\odot}) = 8.98 \pm 0.44$ using eq. 12 in Graham (2007). Aharonian et al. (2007b) give an estimate of $M_{\bullet} = (1 \dots 2) \times 10^9 M_{\odot}$. For a comparative study using values inferred by different methods is not advisable due to possible different systematics. Therefore, the M_{\bullet} value used for PKS 2155-304 should be taken with care in the following. The BH mass of 3C 279 was determined using the virial BH mass estimate of McLure & Dunlop (2002) and is given as $\log(M_{\bullet}/M_{\odot}) = 8.912$ by Gu et al. (2001). It is essentially not used in this study. For two of the blazars under study, PG 1553+113 and 1ES 1101-232, no M_{\bullet} estimations exist yet.

Recent estimations of the BH masses for 452 AGNs find them distributed over a large range of $(10^6 - 7 \times 10^9) M_{\odot}$ with no evidence for dependencies on the radio loudness of the objects (Woo & Urry 2002a,b). A recent study of the BH mass distribution of 66 BL Lac objects (Woo et al. 2005) reports a M_{\bullet} range of $(10^7 - 4 \times 10^9) M_{\odot}$ and could also not find a correlation of M_{\bullet} with radio or X-ray luminosity. (In Sect. 5.5 the distribution of VHE blazars in luminosity and M_{\bullet} is discussed). As Fig. 3 shows, there is no dependence of the BH masses of the VHE blazars on their redshift,

Table 2. Measured velocity dispersions and resulting estimated black hole masses for the VHE blazars.

Object	σ [km s ⁻¹] Ref. 1	$\log(M_{\bullet}/M_{\odot})$	σ [km s ⁻¹] Ref. 2	$\log(M_{\bullet}/M_{\odot})$	σ [km s ⁻¹] Ref. 3	$\log(M_{\bullet}/M_{\odot})$	$\log(M_{\bullet}/M_{\odot})$ averaged
Mkn 421	219 ± 11	8.29 ± 0.18	236 ± 10	8.42 ± 0.15	324 ± 18	8.97 ± 0.12	8.56
Mkn 501	372 ± 18	9.21 ± 0.11	291 ± 13	8.78 ± 0.11	9.00
1ES 2344+514	294 ± 24	8.80 ± 0.15	389 ± 20	9.29 ± 0.12	9.04
Mkn 180	209 ± 11	8.20 ± 0.19	244 ± 10	8.47 ± 0.14	251 ± 16	8.52 ± 0.15	8.40
1ES 1959+650	195 ± 15	8.08 ± 0.23	219 ± 15	8.28 ± 0.19	8.18
BL Lacertae	245 ± 16	8.48 ± 0.15	8.48
PKS 0548-322	202 ± 24	8.14 ± 0.24	8.14
PKS 2005-489	257 ± 16	8.57 ± 0.14	...
H 1426+428	269 ± 16	8.65 ± 0.13	...
H 2356-309	195 ± 14	8.08 ± 0.23	...
1ES 0229+200	363 ± 19	9.16 ± 0.11	...
1ES 1218+304	191 ± 14	8.04 ± 0.24	...
1ES 0347-121	214 ± 15	8.24 ± 0.19	...
1ES 1011+496	219 ± 15	8.28 ± 0.19	...

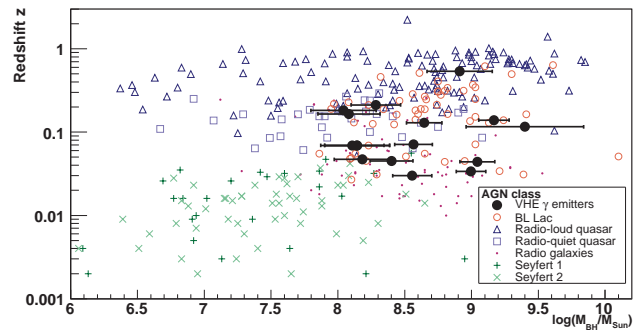
References: (1) Barth, Ho & Sargent (2003); (2) Falomo, Kotilainen & Treves (2002); (3) Wu, Liu & Zhang (2002). The velocity dispersions σ were translated into estimated BH masses using the $M_{\bullet} - \sigma$ relation from Tremaine et al. (2002). The σ values taken from Wu et al. (2002) were indirectly determined using the fundamental plane of radio galaxies (Bettoni et al. 2001). BH masses given in units of the solar mass, M_{\odot} . If more than one M_{\bullet} value is given, the average M_{\bullet} is used. Due to the possible different systematic errors of the individual data sets, the largest error was assumed as error of the average M_{\bullet} .

**Figure 3.** Redshift vs. M_{\bullet} distribution for the known VHE γ -ray emitting AGNs. The superimposed histogram shows the BH mass distribution of the 375 AGNs given in Fig. 4 (linear scale independent of z).

but they are rather flatly distributed in their BH masses between $(10^8 - 10^{9.5})M_{\odot}$. Although AGNs harbour BHs with $M_{\bullet} > 10^6 M_{\odot}$, up to now only blazars with rather massive BHs, $M_{\bullet} \gtrsim 10^8 M_{\odot}$, have been discovered in VHE γ -rays, raising the question whether a physics reason is responsible for the non-detection of less massive blazar BHs in the mass range $(10^7 - 10^8)M_{\odot}$. The BH masses of the VHE blazars are compared to those of 375 AGNs collected by Woo & Urry (2002a) in Fig. 4. The confinement of Seyfert galaxy measurements to low redshifts presumably is due to a selection effect: These are spiral galaxies and therefore expected to harbour comparatively low-mass BHs. Distant Seyfert galaxies ($z \gtrsim 1.0$) might just not be luminous enough to obtain M_{\bullet} measurements. Conversely, quasars are too rare as to be found in small volumes and thus at small distances.

4 INTRINSIC VHE γ -RAY EMISSION PARAMETERS

VHE γ -ray observations enable us to look deep into the emission regions of blazar jets and thus convey information on the responsible particle acceleration and cooling processes. Here we study pri-

**Figure 4.** The redshift vs. M_{\bullet} distribution for 375 AGNs collected by Woo & Urry (2002a) and the known VHE γ -ray emitting AGNs.

marily the differential energy spectra in the VHE domain, which are summarised in Tab. 3. For the sources Mkn 421, Mkn 501, PKS 2155-304, 1ES 1959+650, and 1ES 2344+514 observations of clearly distinct flux states exist. Accordingly, for each of those sources two spectra, one ‘low-state’ and one ‘high-state’ spectrum, are considered. Low-state spectra are characterised by the absence of high ($\gtrsim 0.2$ Crab units¹) flux levels and short-term variability (probably beyond instrumental sensitivity though), while flare spectra were obtained during outbursts of the respective sources (viz. the 1995 December 20 flare of 1ES 2344+514, the 1997 flare of Mkn 501, the 2002 flare of 1ES 1959+650, and the 2006 July 28 flare of PKS 2155-304). At present for none of these sources, even for those with only one flux state, can a true baseline flux state be claimed, although low-flux states have been observed (Albert et al. 2006a, 2007b). Long-term monitoring campaigns are currently performed to address this issue (Goebel et al. 2007; Steele et al. 2007; Punch 2007).

The measured spectra suffer $\gamma\gamma$ absorption on photons of the

¹ The Crab nebula exhibits a strong, constant VHE γ -ray flux and is therefore often considered a standard candle in VHE γ -ray astronomy

Table 3. Measured VHE blazar spectra, reconstructed intrinsic spectral indices and luminosities.

Object	Measured Energy Spectrum dF/dE [$\text{TeV}^{-1} \text{ cm}^{-2} \text{ s}^{-1}$]	Reference	Intrinsic Slope Γ	$\nu_\gamma L_\gamma$ [$\text{erg s}^{-1} \text{ sr}^{-1}$]
Mkn 421	$(12.1 \pm 0.5)10^{-12}(E/1.0 \text{ TeV})^{-3.09 \pm 0.07}$	Aharonian et al. (1999b)	2.85 ± 0.58	$(9.68 \pm 0.40) \times 10^{43}$
Mkn 501	$(8.4 \pm 0.5)10^{-12}(E/1.0 \text{ TeV})^{-2.76 \pm 0.08}$	Aharonian et al. (2001b)	2.49 ± 0.84	$(6.89 \pm 0.41) \times 10^{43}$
1ES 2344+514	$(1.2 \pm 0.2)10^{-11}(E/0.5 \text{ TeV})^{-2.95 \pm 0.12}$	Albert et al. (2007b)	2.67 ± 0.21	$(2.80 \pm 0.47) \times 10^{43}$
Mkn 180	$(4.5 \pm 1.8)10^{-11}(E/0.3 \text{ TeV})^{-3.3 \pm 0.7}$	Albert et al. (2006c)	3.06 ± 0.50	$(2.04 \pm 0.81) \times 10^{43}$
1ES 1959+650	$(3.4 \pm 0.5)10^{-12}(E/1.0 \text{ TeV})^{-2.72 \pm 0.14}$	Albert et al. (2006a)	2.37 ± 0.29	$(5.95 \pm 0.88) \times 10^{43}$
BL Lacertae	$(1.9 \pm 0.5)10^{-11}(E/0.3 \text{ TeV})^{-3.64 \pm 0.54}$	Albert et al. (2007d)	3.17 ± 0.25	$(2.35 \pm 0.62) \times 10^{43}$
PKS 0548-322	$(1.9 \pm 0.4)10^{-13}(E/1.0 \text{ TeV})^{-2.8 \pm 0.3}$	Superina et al. (2007)	2.38 ± 0.28	$(9.66 \pm 2.05) \times 10^{42}$
PKS 2005-489	$(1.9 \pm 0.7)10^{-13}(E/1.0 \text{ TeV})^{-4.0 \pm 0.4}$	Aharonian et al. (2005b)	3.52 ± 0.27	$(2.53 \pm 0.93) \times 10^{43}$
PKS 2155-304	$(1.96 \pm 0.12)10^{-12}(E/1.0 \text{ TeV})^{-3.32 \pm 0.06}$ for $E < 700 \text{ GeV}$, $(2.4^{+0.4}_{-0.3})10^{-12}(0.7 \pm 0.2)^{(3.79^{+0.46}_{-0.27}-3.15^{+0.10}_{-0.12})}$ for $E > 700 \text{ GeV}$	Aharonian et al. (2005a)	2.43 ± 0.64	$(6.32 \pm 0.39) \times 10^{44}$
H 1426+428	$(2.9 \pm 1.1)10^{-11}(E/0.43 \text{ TeV})^{-2.6 \pm 0.6}$	Horan & Finley (2001), Aharonian et al. (2002)	1.58 ± 0.23	$(7.42 \pm 2.81) \times 10^{44}$
1ES 0229+200	$(2.34 \pm 0.37)10^{-14}(E/3.0 \text{ TeV})^{-2.5 \pm 0.2}$	Raue et al. (2007)	1.39 ± 0.30	$(6.13 \pm 0.98) \times 10^{43}$
H 2356-309	$(3.08 \pm 0.75)10^{-13}(E/1.0 \text{ TeV})^{-3.06 \pm 0.4}$	Aharonian et al. (2006a)	1.77 ± 0.37	$(3.29 \pm 0.80) \times 10^{44}$
1ES 1218+304	$(8.1 \pm 2.1)10^{-11}(E/0.25 \text{ TeV})^{-3.0 \pm 0.4}$	Albert et al. (2006b)	1.97 ± 0.40	$(1.26 \pm 0.33) \times 10^{45}$
1ES 1101-232	$(4.44 \pm 0.74)10^{-13}(E/1.0 \text{ TeV})^{-2.88 \pm 0.14}$	Aharonian et al. (2006a)	1.33 ± 0.37	$(3.19 \pm 0.53) \times 10^{44}$
1ES 0347-121	$(4.52 \pm 0.85)10^{-13}(E/1.0 \text{ TeV})^{-3.10 \pm 0.23}$	Aharonian et al. (2007c)	1.76 ± 0.14	$(3.19 \pm 0.60) \times 10^{44}$
1ES 1011+496	$(2.0 \pm 0.1)10^{-10}(E/0.2 \text{ TeV})^{-4.0 \pm 0.5}$	Albert et al. (2007e)	2.56 ± 0.29	$(15.4 \pm 0.77) \times 10^{44}$
PG 1553+113 ^a	$(1.8 \pm 0.3)10^{-10}(E/0.2 \text{ TeV})^{-4.21 \pm 0.25}$	Albert et al. (2007a)	3.68 ± 0.68	$(6.40 \pm 1.07) \times 10^{43}$
PG 1553+113 ^b	$(1.8 \pm 0.3)10^{-10}(E/0.2 \text{ TeV})^{-4.21 \pm 0.25}$	Albert et al. (2007a)	2.34 ± 0.46	$(3.14 \pm 0.52) \times 10^{45}$
Mkn 421 ^c	$(23.40 \pm 0.73)10^{-11}(E/1.0 \text{ TeV})^{-2.32 \pm 0.03}$	Krennrich et al. (2002)	2.09 ± 0.30	$(1.08 \pm 0.03) \times 10^{45}$
Mkn 501 ^c	$(2.50 \pm 0.16)10^{-10}(E/1.0 \text{ TeV})^{-2.22 \pm 0.04}$	Aharonian et al. (1999a)	1.95 ± 0.41	$(1.39 \pm 0.09) \times 10^{45}$
1ES 2344+514 ^c	$(5.1 \pm 1.0)10^{-11}(E/1.0 \text{ TeV})^{-2.54 \pm 0.17}$	Schroedter et al. (2005)	2.20 ± 0.31	$(6.65 \pm 1.30) \times 10^{44}$
1ES 1959+650 ^c	$(1.23 \pm 0.25)10^{-10}(E/1.0 \text{ TeV})^{-2.78 \pm 0.12}$	Daniel et al. (2005)	2.43 ± 0.29	$(2.25 \pm 0.46) \times 10^{45}$
PKS 2155-304 ^c	$(2.06 \pm 0.16)10^{-10}(E/1.0 \text{ TeV})^{-2.71 \pm 0.06}$ for $E < 340 \text{ GeV}$, $(2.06 \pm 0.16)10^{-10}(0.430 \pm 0.022)^{(3.53 \pm 0.05)-(2.71 \pm 0.06)}$ for $E > 340 \text{ GeV}$	Aharonian et al. (2007b)	2.28 ± 0.40	$(2.74 \pm 0.17) \times 10^{46}$

Γ denotes the reconstructed (intrinsic) VHE spectral power-law index at 500 GeV and $\nu_\gamma L_\gamma$ represents the source luminosity at 500 GeV. Both values were calculated from the measured spectra assuming a Kneiske et al. ‘low-IR’ EBL density. ^a at an assumed $z = 0.1$. ^b at an assumed $z = 0.3$. ^c spectrum measured during a flare state of the respective blazar.

EBL as shown in Sect. 2. The intrinsic source spectra are reconstructed employing (Mazin 2003) the EBL ‘low-IR’ model given in Kneiske et al. (2004), which assumes the least possible infrared star formation rate as allowed by galaxy counts and which is in reasonable agreement with other models (Primack, Bullock & Somerville 2005; Stecker, Malkan & Scully 2006). Note that due to the fact that the VHE γ -rays are attenuated exponentially with the optical depth, an accurate knowledge is crucial for the individual interpretation of the intrinsic VHE γ -ray spectra.

In the following, we will use two observables to characterise the VHE γ -ray emission: The K -corrected (Hogg et al. 2002) luminosity at 500 GeV, $\nu_\gamma L_\gamma = 4\pi d_L^2 \cdot (500 \text{ GeV})^2 F(500 \text{ GeV}/(1+z))/(1+z)$ with the luminosity distance d_L and the intrinsic photon index Γ in the region around 500 GeV, which is determined by fitting the intrinsic spectra with pure power laws of the form $dF/dE = f_0 \cdot (E/E_0)^{-\Gamma}$. These two parameters act as proxies for the peak position and the spectra shape on the falling edge of the high-energy bump, which cannot, as earlier explained, easily be determined from the existing VHE data. For extraction of the luminosity and of the spectral slope the region around 500 GeV was chosen because all blazars under study have measured spectra in this energy region. All calculations and fits have been performed in energy ranges where γ -ray spectra for the respective blazars have actually been observed, so that no extrapolations in energy regions not covered by the data were required. All in all, extragalactic

source observations included in this paper cover the energy range $85 \text{ GeV} \leq E \leq 11 \text{ TeV}$. For the determination of the luminosity distances the cosmological parameters given in Spergel et al. (2007) were used: $\Omega_m h^2 = 0.127^{+0.007}_{-0.013}$, $\Omega_b h^2 = 0.0223^{+0.0007}_{-0.0009}$ with the Hubble constant $H_0 = 100 \cdot h \text{ km s}^{-1} \text{ Mpc}^{-1} = 73^{+3}_{-3} \text{ km s}^{-1} \text{ Mpc}^{-1}$.

Tab. 3 also shows the resulting source luminosities in the VHE region and the spectral slope of the reconstructed source-intrinsic spectra. While the luminosities range from $\approx 10^{43} \text{ erg s}^{-1} \text{ sr}^{-1}$ to $\approx 3 \times 10^{45} \text{ erg s}^{-1} \text{ sr}^{-1}$ ($\approx 10^{45} \text{ erg s}^{-1} \text{ sr}^{-1}$ to $\approx 3 \times 10^{46} \text{ erg s}^{-1} \text{ sr}^{-1}$ for blazars in outburst), the photon indices of the reconstructed intrinsic spectra vary between $\Gamma = 1.4 - 3.3$, except for 1ES 1101-232, which probably has an intrinsic spectrum peaking far beyond $E = 1 \text{ TeV}$ (Aharonian et al. 2007a). The VHE measurements lie close to, but generally above the maximum of the high-energy bump (which occurs at $\Gamma = 2$). Spectra with $\Gamma < 1.5$ are difficult to explain in current acceleration models (Malkov & Drury 2001; Aharonian et al. 2006a; but see Katarzyński et al. 2006a,b for models that would explain harder spectra). The rather hard intrinsic slopes found for some sources go in line with indications that the EBL absorption effects are still smaller than currently modelled (e.g., Aharonian et al. 2006a): a lower EBL level would soften the intrinsic spectra inferred here, i.e. increase the value of Γ .

Before instruments like MAGIC and H.E.S.S. became operational, the average observed photon index in BL Lac objects was $\Gamma \approx 2.3$. This raised the expectation that AGNs would in

general exhibit rather hard spectra in the VHE range, which also would be compatible with the average EGRET blazar spectrum (at MeV-GeV energies) found to have a slope of $\Gamma_{\text{EGRET}} = 2.27$ (Venters & Pavlidou 2007). In fact, the average spectral slope at VHE has not changed much, although the scatter on Γ increased as a new population of objects with intrinsically rather soft spectra (Mkn 180, PKS 2005-489) has been tapped, and at the same time distant, hard-spectra sources were found.

For PG 1553+113 with its unknown redshift, two possible distances ($z = 0.1$, $z = 0.3$) were assumed in this paper. The resulting ‘intrinsic spectra’, however, are only given for illustrative purposes and are not used for any conclusions throughout this study unless stated otherwise.

5 CORRELATION STUDIES

5.1 Correlation of X-ray, optical, radio, and VHE γ -ray luminosity

In SSC models, the X-ray and the VHE emissions are closely connected, owing to their common origin. While in some blazars clear evidence for a corresponding correlation has been observed (Mkn 421, Krawczynski et al. 2001; Błażejowski et al. 2005; Albert et al. 2007c), the connection is only weak for other ones (Mkn 501, Albert et al. 2007f) or even non-existing during some flare states (the IES 1959+650 *orphan flare* case, Daniel et al. 2005). Fig. 5 shows $\nu_\gamma L_\gamma$ versus the X-ray luminosity at 1 keV ($\nu_X L_X$; from Costamante & Ghisellini 2002). Note that high thermal contributions at 1 keV are unlikely and would imply a very high amount of gas and pressure. Unfortunately, the X-ray and VHE data points have not been taken simultaneously. While VHE measurements during outbursts were not used in the Figure, variations in the X-ray domain for the blazars under study are, according to the compilation of X-ray fluxes in Donato et al. (2001), not larger than a factor 4.6 (most extreme object: Mkn 501) with an average of a factor 1.4 and a variance of 2.2. According to expectations, a trend towards a correlation is visible. When including all data points except for those representing PG 1553+113, we find a correlation coefficient of $r = 0.76^{+0.09}_{-0.14}$, which is within 3.6 standard deviations different from zero. A linear fit to the data yields a slope of $m = 1.11 \pm 0.09$ ($\chi^2_{\text{red}} = 61.8/14$).

Recently, optical triggers lead to the successful discoveries of the VHE blazars Mkn 180 (Albert et al. 2006c) and IES 1011+496 (Albert et al. 2007e). At times of lower optical emission the latter in fact showed a lower flux and thus only yielded a marginal detection (Albert et al. 2007g). This seems to imply the existence of a VHE – optical connection, which would be a convenient proxy for finding new VHE blazars. However, in the past no (Błażejowski et al. 2005; Rebillot et al. 2006; Albert et al. 2007a) or only weak (Buckley et al. 1996) evidence for optical or radio to VHE correlations was found for individual observations of Mkn 421 and PG 1553+113.

The optical flux data at 5500 Å used here were collected from several source catalogues by Costamante & Ghisellini (2002), as were the radio flux data at 5 GHz. We converted them into luminosities taking into account the appropriate luminosity distances d_L . Fig. 6 shows the corresponding correlations: the data in the VHE – optical plane feature a larger scatter than that in the VHE – X-ray data, while in the VHE – radio plane no clear trend is seen.

VHE blazars might populate only restricted ranges in X-ray, optical, or radio luminosity distributions. To test this, we use X-

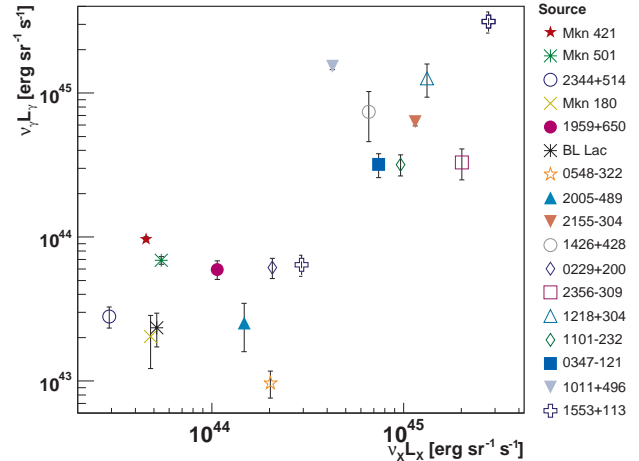


Figure 5. VHE γ -ray luminosity $\nu_\gamma L_\gamma$ vs. X-ray luminosity at 1 keV, $\nu_X L_X$ for 17 VHE blazars. The two data points for PG 1553+113 (open crosses) are for assumed redshifts of $z = 0.1$ ($\nu_\gamma L_\gamma = 6.4 \times 10^{43} \text{ erg sr}^{-1} \text{ s}^{-1}$) and $z = 0.3$ ($\nu_\gamma L_\gamma = 3.1 \times 10^{45} \text{ erg sr}^{-1} \text{ s}^{-1}$), respectively, and are not used in the fit and for determining the correlation coefficient (see text). It should be noted that VHE data points have an additional systematic error of typically 35 per cent. The systematic error of the X-ray luminosities is unfortunately unknown.

ray, optical, and radio data from the full set of 246 sources considered by Costamante & Ghisellini (2002). We rejected the sources for which no redshift is known and converted the remaining 183 fluxes into luminosities. These blazars are compared to the VHE blazars in Fig. 7. In none of the three distributions can substantial deviations of the VHE blazars from the overall set of blazars be found.

5.2 Correlations of intrinsic photon index and VHE luminosity with the synchrotron peak frequency

In SSC models the VHE peak, identified with the inverse Compton (IC) peak with a maximum at $\nu_{\text{peak}}^{\text{IC}}$, resembles the form (e.g., Fossati et al. 1998) of the synchrotron peak at $\nu_{\text{peak}}^{\text{Sy}}$, displaced by the squared Lorentz factor $\nu_{\text{peak}}^{\text{IC}}/\nu_{\text{peak}}^{\text{Sy}} \sim \gamma^2$ (Tavecchio et al. 1998). Nieppola, Tornikoski & Valtaoja (2006) collected (non-simultaneous) multiwavelength data for a large (> 300) set of blazars, which includes eleven of the VHE blazars under study here. The data, covering frequencies from the 5 GHz radio to the 2.4 keV X-ray domain, were used by Nieppola et al. to reconstruct the SEDs of these blazars and to infer the synchrotron peak frequency $\nu_{\text{peak}}^{\text{Sy}}$. We test for correlations between $\nu_{\text{peak}}^{\text{Sy}}$ and the VHE luminosity and spectral slope (Fig. 8). According to expectations from SSC models, we find a correlation of the photon index Γ with $\nu_{\text{peak}}^{\text{Sy}}$. The correlation coefficient is given as $r = -0.63^{+0.28}_{-0.18}$ and a linear fit to the data as shown in Fig. 8a yields a $\chi^2_{\text{red}} = 12.1/8$. Fig. 8b shows the corresponding data points in the $\nu_\gamma L_\gamma - \nu_{\text{peak}}^{\text{Sy}}$ plane, in which no correlation is apparent. Finally, in Fig. 9, we check whether the LBL–HBL transition of the VHE blazars is connected with the BH masses of their host galaxies. Ten of the VHE blazars, for which both $\nu_{\text{peak}}^{\text{Sy}}$ and M_* measurements are available, show no trend towards a correlation.

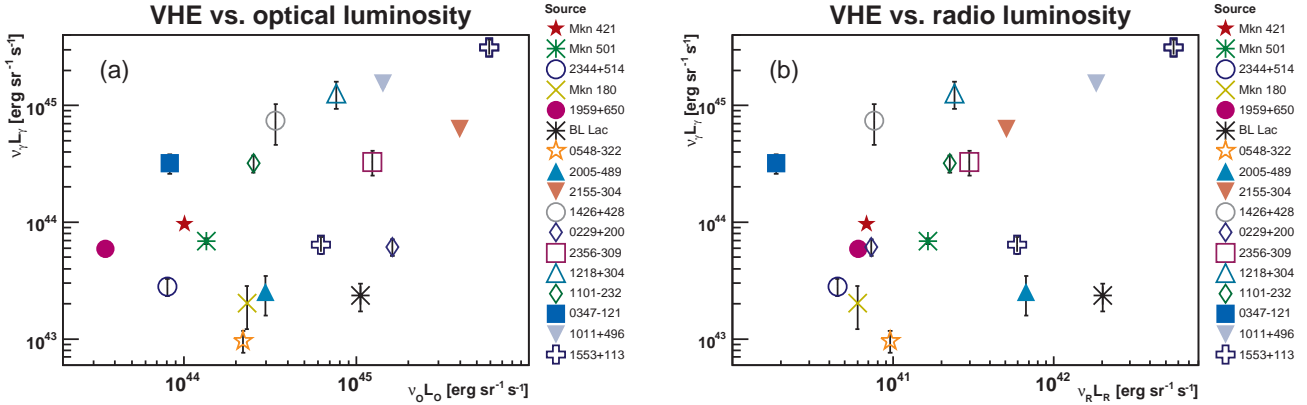


Figure 6. (a) Correlation of VHE luminosity $\nu_\gamma L_\gamma$ and optical luminosity $\nu_O L_O$. (b) Correlation of VHE luminosity $\nu_\gamma L_\gamma$ and radio luminosity $\nu_R L_R$. The two data points for PG 1553+113 (open crosses) are for assumed redshifts of $z = 0.1$ ($\nu_\gamma L_\gamma = 6.4 \times 10^{43} \text{ erg sr}^{-1} \text{ s}^{-1}$) and $z = 0.3$ ($\nu_\gamma L_\gamma = 3.1 \times 10^{45} \text{ erg sr}^{-1} \text{ s}^{-1}$), respectively.

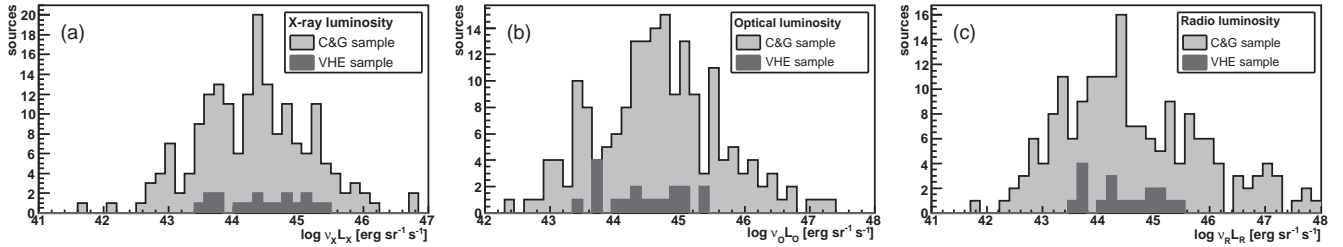


Figure 7. Histograms of (a) 1 keV X-ray, (b) 5500 Å optical, and (c) 5 GHz radio luminosity of the VHE blazars and all those blazars considered by Costamante & Ghisellini (2002) with determined redshifts (183 out of the total set of 246 blazars).

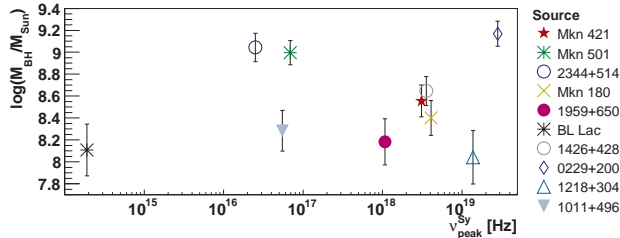


Figure 9. Estimated BH mass vs. synchrotron peak frequency $\nu_{\text{peak}}^{\text{Sy}}$ for those VHE blazars with both quantities known.

5.3 Correlation between the intrinsic photon index and the VHE γ -ray luminosity

Fig. 10a relates the intrinsic photon indices Γ to the VHE γ -ray luminosities $\nu_\gamma L_\gamma$. For all objects under study (excluding flare states and the PG 1553+113 data), the $\Gamma - \nu_\gamma L_\gamma$ correlation reads as $\Gamma = \Gamma_0 + m \cdot \log_{10}(\nu_\gamma L_\gamma)$ with $\Gamma_0 = 38.5 \pm 6.8$ and $m = -0.82 \pm 0.15$. The fit which led to this correlation has a $\chi^2_{\text{red}} = 40.18/14$. The line at $\Gamma = 2$ denotes the spectral slope at which a maximum in the SED occurs. Looking at the spread of the observations in Γ as a function of $\nu_\gamma L_\gamma$, we notice that the distribution sharpens towards $\Gamma = 2$. This might reflect that the highest luminosity occurs at $\Gamma = 2$. Thus the spread of the data reflects the spread of the shapes of the high energy peaks. The general behaviour above $\Gamma \approx 2$ – the higher the VHE γ -ray luminosity, the harder the spectrum – can within SSC models be described with a moving IC peak towards higher energies with increasing luminosity. The five blazars with observed spectra at quiescent and flare states partially be-

have in a similar manner (Fig. 10b): Mkn 421 (Krawczynski et al. 2001; Błażejowski et al. 2005), Mkn 501 (Albert et al. 2007f), and 1ES 2344+514 (Albert et al. 2007b) also show a spectral hardening during high-flux states, flares, and outbursts. Fig. 11a shows the corresponding luminosity differences $\Delta(\nu_\gamma L_\gamma)$ and slope differences $\Delta\Gamma$. Mkn 501 and 1ES 2344+514 show a similar change in spectral slope and a dynamical range of $\Delta(\nu_\gamma L_\gamma) \approx 20$. The luminosity increase of Mkn 421 observed up to now is much lower with $\Delta(\nu_\gamma L_\gamma) \approx 10$. While the spectral slope of Mkn 421 also hardens with increasing luminosity, 1ES 1959+650 and PKS 2155-304 show within errors no variation in their spectral slopes during flares, while their luminosities increase rather drastically by a factor of 40 and 50, respectively. When plotting the luminosity difference versus the BH masses (Fig. 11b), a trend, although broken by 1ES 1959+650, towards blazars with more massive BHs showing higher dynamical ranges of their emission, is found.

5.4 A test for selection effects: redshift dependencies?

Possible correlations of Γ and $\nu_\gamma L_\gamma$ with the redshift z are not expected, but may identify selection effects in the data set and/or an inaccurate EBL model. Conspicuously, very hard ($\Gamma \ll 2.0$) spectra have up to now been only reconstructed for rather distant ($z \gtrsim 0.1$) blazars (Fig. 12a). At the same time, none of the measured spectra of nearby sources shows Γ much smaller than 2.0, although for these blazars no strong EBL modifications apply and the measured spectra should not differ substantially from the intrinsic ones in the energy region studied here. Why are only blazars with rather hard intrinsic spectra visible at large distances ($z > 0.1$)? Soft spectra

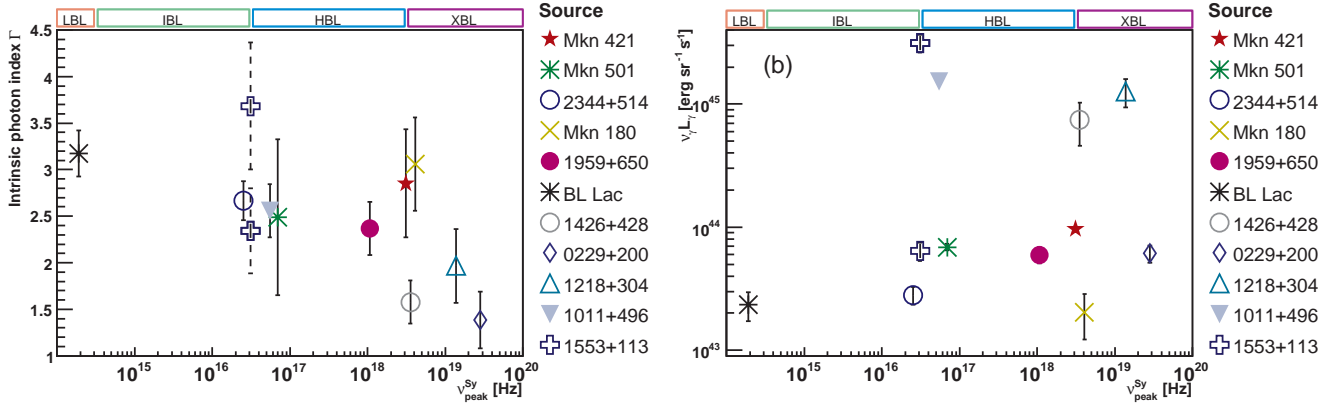


Figure 8. (a) Photon index Γ vs. synchrotron peak frequency $\nu_{\text{peak}}^{\text{Sy}}$ and (b) VHE luminosity vs. synchrotron peak frequency $\nu_{\text{peak}}^{\text{Sy}}$ for eleven VHE blazars. The synchrotron peak frequencies and the LBL-IBL-HBL classification are taken from Nieppola et al. (2006). The two data points for PG 1553+113 (open crosses) are for assumed redshifts of $z = 0.1$ ($\Gamma = 3.68 \pm 0.68$; $\nu_{\gamma} L_{\gamma} = 6.4 \times 10^{43} \text{ erg sr}^{-1} \text{ s}^{-1}$) and $z = 0.3$ ($\Gamma = 2.34 \pm 0.46$; $\nu_{\gamma} L_{\gamma} = 3.1 \times 10^{45} \text{ erg sr}^{-1} \text{ s}^{-1}$), respectively, and are not used in the fit and for determining the correlation coefficient in the left Figure (a).

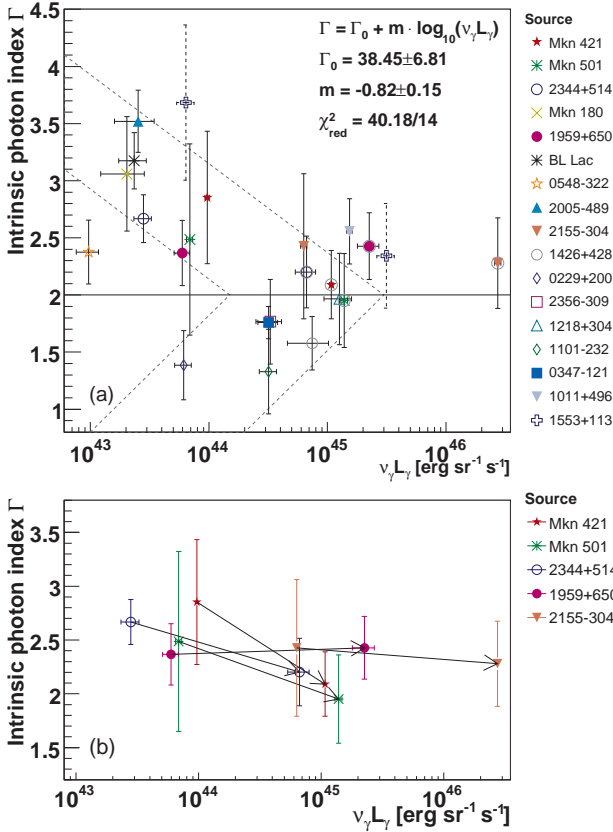


Figure 10. (a) Intrinsic photon index vs. luminosity. Additional flare states of sources are marked by grey circles. The results of a linear fit of the form $\Gamma = \Gamma_0 + m \log_{10}(\nu_{\gamma} L_{\gamma})$ are given in the figure. The two data points for PG 1553+113 (open crosses), not included in this fit, are for assumed redshifts of $z = 0.1$ (low luminosity) and $z = 0.3$ (high luminosity), respectively. (b) As before, but only for the five blazars for which low and high VHE γ flux states have been observed.

certainly fall more easily below the current instrumental sensitivity limits. Another explanation for the prevalent hard spectra at large z is an overcorrection of the EBL attenuation effects.

Fig. 12b shows the corresponding distribution of VHE lumi-

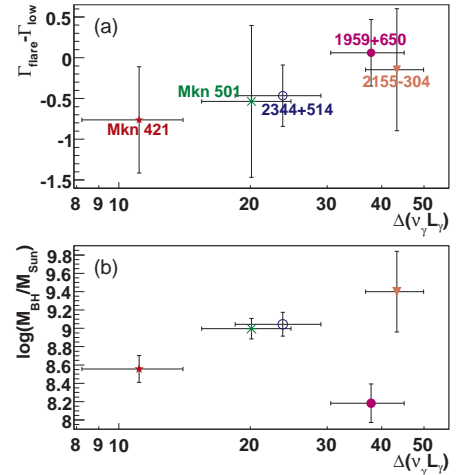


Figure 11. (a) Evolution of intrinsic spectral index Γ and source luminosity from low to high VHE γ flux states: luminosity ratio $\Delta(\nu_{\gamma} L_{\gamma}) = (\nu_{\gamma} L_{\gamma})_{\text{flare}} / (\nu_{\gamma} L_{\gamma})_{\text{low}}$ versus the difference of intrinsic photon indices. (b) Luminosity ratio $\Delta(\nu_{\gamma} L_{\gamma}) = (\nu_{\gamma} L_{\gamma})_{\text{flare}} / (\nu_{\gamma} L_{\gamma})_{\text{low}}$ versus M_{\bullet} .

nosities $\nu_{\gamma} L_{\gamma}$ as a function of z . Two curves indicate the sensitivity limit of current IACTs (e.g., Aharonian et al. 2006b), a significant detection of 1 per cent of the flux of a Crab nebula-like source in 25 hours, and the sensitivity of previous (< 2002) IACTs of ≈ 10 per cent of this flux. Interestingly, most of the sources found at $z > 0.05$ seem to be rather low-luminosity sources in the sense that their luminosity is not much higher than the current instrumental sensitivity allows for. This means that not only the substantially lower energy thresholds of the current IACTs ($\lesssim 100$ GeV as compared to ≈ 300 GeV until 2004), but also their increased sensitivity enabled some of the new blazar discoveries. Exceptions to these detections close to the current sensitivity limit are (trivially) the six VHE blazars discovered before 2002, 1ES 1011+496 (but discovered during an optical flare, while its low-flux state seems to lie below the current instrumental reach, Albert et al. 2007e,g), and 1ES 1218+304, which in fact seems to have been detected in a non-flare state. Note further that H 1426+428 has not yet been detected after 2002 (e.g., Albert et al. 2007g), which also currently places it below sensitivity limits.

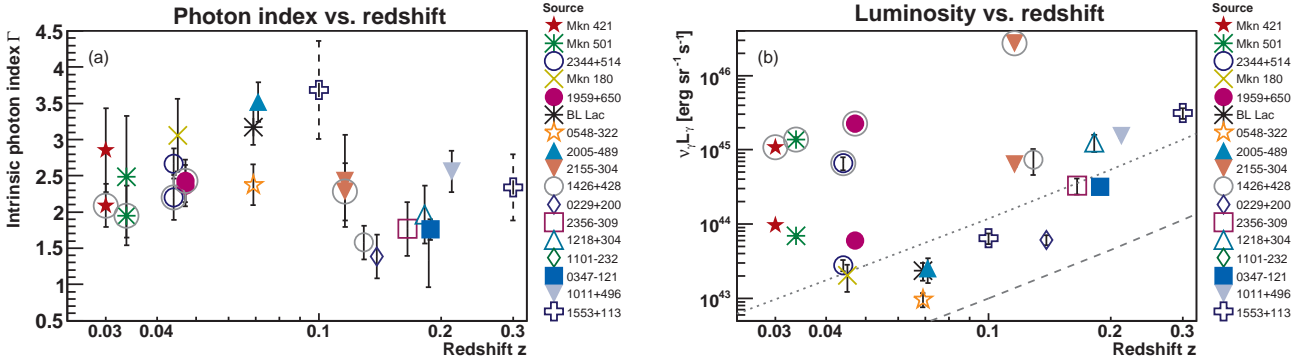


Figure 12. Correlations of redshift with (a) the intrinsic photon index and (b) VHE γ -ray luminosity. For Mkn 421, Mkn 501, 1ES 2344+514, PKS 2155-304, and 1ES 1959+650 flare flux levels are also included in the plots; the corresponding data points are marked by additional grey circles. The two data points for PG 1553+113 (open crosses) are for assumed redshifts of $z = 0.1$ and $z = 0.3$, respectively. The dashed curve in the right Figure (b) marks the sensitivity (e.g., Aharonian et al. 2006b) limit of current IACTs (selection effect); the dotted line indicates the sensitivity of previous (< 2002) IACTs.

5.5 Correlations of intrinsic VHE γ -ray emission parameters with the black hole mass

The γ -ray production is thought to take place at shock fronts inside the AGN jets at very close (sub-parsec) distances from the central BH (Jester et al. 2006; Uchiyama et al. 2006). While the jet production and collimation mechanism is still elusive, accepted models are generally based on magnetohydrodynamic (Blandford & Payne 1982; Kudoh et al. 1999) or electromagnetic jet models. In the latter, a Poynting flux dominated flow is launched from a Kerr BH (Blandford & Znajek 1977) or from the accretion disc (Blandford 1976). The conversion from Poynting dominance into particle dominance is not yet understood. The properties of the blazar γ -ray emission are expected to be connected to the properties of the central BH, like M_\bullet and the BH spin, since scaling laws govern BH physics (McHardy et al. 2006), in particular length and time scales of flows (Mirabel & Rodríguez 1999; Mirabel 2004), e.g. the orbital period of the last stable BH orbit. Currently, only M_\bullet can be reliably estimated; the BH spin remains inaccessible by large. Moreover, the environment in which the BH is embedded might be equally important; one of its properties, the accretion rate, is indirectly accessible through the (radio) jet power, which, however, cannot be measured for blazars (Liu et al. 2006). A previous study of the connection of spectral properties and M_\bullet for five VHE blazars (Krawczynski et al. 2004) did not find any correlations to the BH mass.

For 15 VHE blazars with known BH masses, we neither find a correlation between M_\bullet and the spectral slope Γ (Fig. 13a), nor between M_\bullet and the VHE γ -ray luminosity (Fig. 13b). Although the uncertainties of the M_\bullet determination are still rather large, the VHE blazar set disfavors a dependency of the VHE γ -ray emission properties studied here on M_\bullet . These properties may more sensitively depend on the BH spin or the accretion rate. The acceleration region in the jet rather than the BH might more dominantly influence the VHE emission properties. Also results on timing properties (see Sect. 5.7) support such claims.

5.6 An upper distance limit for PG 1553+113

The redshift determination for blazars is challenging, as these AGNs generally exhibit only weak spectral lines. In several attempts, no emission or absorption lines could be found in the optical/IR spectrum of PG 1553+113; see, e.g., Wagner et al.

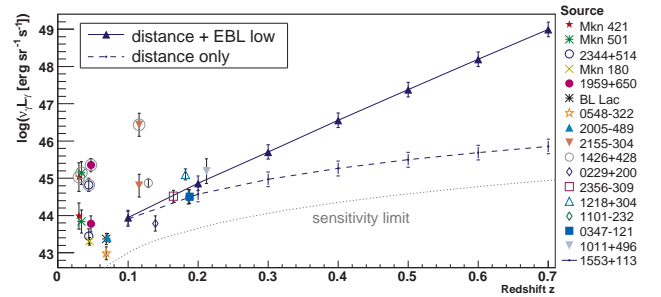


Figure 14. Luminosity evolution for PG 1553+113 assumed at different distances. Together with the luminosities of the other known VHE γ -ray emitting blazars, the luminosity of PG 1553+113 as a function of its assumed distance is shown. The solid curve includes both the distance and the EBL attenuation effect, the latter calculated using the ‘low IR’ model given in Kneiske et al. (2004). The dashed curve illustrates how weak the effect only by increasing the distance is. The dotted curve indicates the current IACT sensitivity limit neglecting EBL attenuation effects. Blazars in flaring state, marked with additional gray circles, were ignored for determining the redshift limit (see text).

(2007) for results of a recent Very Large Telescope (VLT) observation campaign. The frequently cited initial determination of $z = 0.36$ (Miller & Green 1983) was found to be based on a misidentified emission line and could not be reproduced (Falomo & Treves 1990; Falomo, Scarpa & Bersanelli 1994). VLT optical spectroscopy (Sbarufatti et al. 2006) yields a lower limit of $z > 0.09$, while the analysis of Hubble Space Telescope images leads to the prediction of a redshift in the range of $z = 0.3 - 0.4$ (Treves, Falomo & Uslenghi 2007). Indirect methods employing the maximum slope (Aharonian et al. 2006b; Albert et al. 2007a) or the shape (Mazin & Goebel 2007) of the VHE γ -ray spectrum find upper limits of $z < 0.74$ and $z < 0.42$, respectively.

With increasing distance, the luminosity of PG 1553+113 has to increase stronger than quadratic due to EBL $\gamma\gamma$ absorption as to sustain the measured VHE flux. Fig. 14 shows the source luminosity (1) when only considering the distance effect and (2) when also taking into account the EBL absorption. Due to the exponential behaviour of the EBL attenuation, the latter effect is by far dominant. We assume here that PG 1553+113 is an ‘off the shelf’ blazar, i.e. with no extraordinarily high luminosity $\nu_\gamma L_\gamma$. This assumption is difficult to quantify; given that the overall dynamical

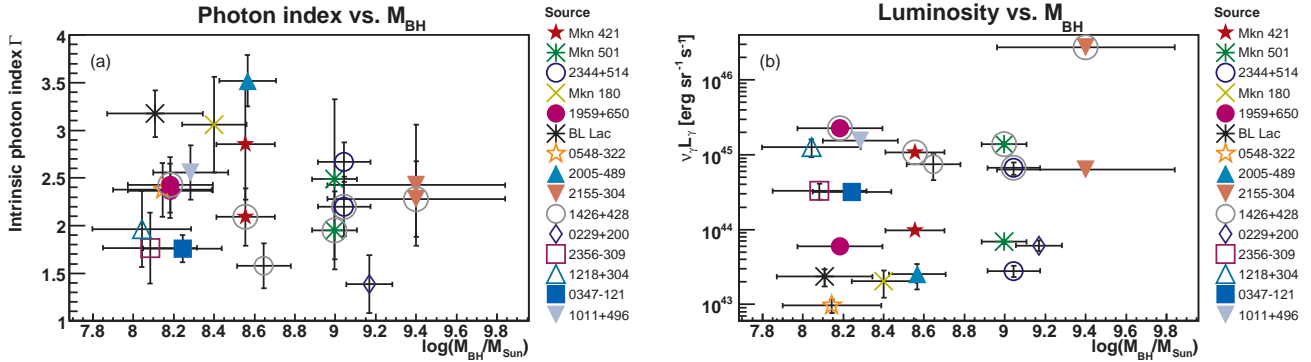


Figure 13. Correlations of black hole mass with (a) the intrinsic photon index and (b) VHE γ -ray luminosity. For Mkn 421, Mkn 501, 1ES 2344+514 and 1ES 1959+650 flare flux levels are also included in the plots; the corresponding data points are marked by additional grey circles.

range of the (non-flare) blazar luminosities in this study of ≈ 75 , we consider the case in which the luminosity of PG 1553+113 is not more than 30 (1000) times higher than the highest luminosity found in the sample. Further, PG 1553+113 has in two years of observations not shown any apparent flaring behaviour; within a factor of three, the measured flux was constant (Aharonian et al. 2006b; Albert et al. 2007a; Benbow et al. 2007). Therefore we consider only sources in non-flare states, of which 1ES 1218+304 with $\nu_\gamma L_\gamma = 1.3 \times 10^{45} \text{ erg s}^{-1} \text{ sr}^{-1}$ is the most luminous one. A 30-times higher luminosity then implies a limit of $z < 0.45$, while an extreme luminosity of $\nu_\gamma L_\gamma = 1.3 \times 10^{48} \text{ erg s}^{-1} \text{ sr}^{-1}$ yields a limit of $z < 0.64$. These limits do not only depend on a good knowledge of the EBL attenuation over a wide range in redshift, but also on the assumed maximum VHE blazar luminosity that strongly depends on the Doppler factor δ . In any case, either a strikingly high luminosity or a very high δ is needed to explain the observations should PG 1553+113 be more distant than $z \gtrsim 0.35$. Note that $\delta \lesssim 20$ suffices for most of the blazars modeled up to now during non-outburst times, as also for flare observations (e.g. Mkn 421, Maraschi et al. 1999). SSC modelling for PG 1553+113 resulted in $\delta = 21$ (Costamante & Ghisellini 2002; Albert et al. 2007a).

The difficulties in finding emission and absorption lines might indicate a very close alignment of the jet axis of PG 1553+113 to our line of sight. Very-long baseline interferometry (VLBI) imaging is available for some VHE HBLs detected before 2002 (Piner et al. 1999; Edwards & Piner 2002; Piner & Edwards 2004) and for BL Lacertae (Denn, Mutel & Marscher 2000), while additional measurements of the recently found VHE blazars are underway (Piner, Pant & Edwards 2007). VLBI essentially confirms the close alignment of the jet to our line of sight on sub-parsec scale and finds opening angles of typically few degrees. These results cannot yet be used for quantitative correlation studies though.

We have to eventually consider the possibilities that PG 1553+113 is a rather distant source and the blazar populations at large distances show significantly different properties than the close-by objects at $z < 0.2$, and that such very extreme objects are so rare that a sufficiently large volume had to be probed to find one of them.

5.7 Correlations with the X-ray duty cycle and the VHE variability time-scale

Following a method described in Krawczynski et al. (2004), we determine the time fraction (‘duty cycle’, DC) for which the (2 – 10) keV X-ray flux exceeds the average flux by 50 per cent. In

this paper, for a blazar to be regarded ‘on duty’ we additionally require this deviation to be significant on the 3σ level. 2–10 keV X-ray light curves are obtained from the All-Sky Monitor detector² on board the Rossi X-ray Timing Explorer (RXTE) and are available from 1996 January 5 on. Fig. 15 shows the corresponding light curves along with the resulting DCs. Objects which are classified as extreme BL Lacs (Mkn 501, 1ES 2344+514, H 1426+428, H 2356-309 and PKS 0548-322, Costamante et al. 2001) show substantially higher activity than the other blazars. Note, however, the outstanding role of Mkn 421 with its substantially higher duty cycle as compared to all other objects. Fig. 16a shows the duty cycle as a function of the BH mass for the VHE blazars. No trends are visible, except for the observation that the three blazars with the most massive BHs ($\log(M_*/M_\odot) > 8.8$) do not have duty cycles in excess of 17 per cent. This goes in line with a speculation of a connection between the X-ray flare duty cycle and M_* seen in the five VHE blazars studied in Krawczynski et al. (2004). The distribution of the X-ray duty cycle as a function of luminosity is found to be rather flat (Fig. 16b), supporting the claim that variability on all scales is a defining property of blazars. Note, however, that Mkn 501 and PKS 2155-304, the objects which show the fastest variability in VHE γ -rays, are among the objects with a rather low duty cycle.

Blazars are characterised by a highly variable emission. In particular the VHE γ -ray emission is often found to be more variable than the emission at other wavelengths. Still, comprehensive data on the temporal behaviour of VHE blazar emission has often been collected only for blazars in outburst, and thus, over short time spans. Although VHE light curves ranging over ten years’ worth of measurements were collected occasionally (e.g. Albert et al. 2007b; Tluczykont et al. 2007; Albert et al. 2007f), the sampling is only sparse, and continuous, unbiased long-term monitoring campaigns have not been started until 2005 (Goebel et al. 2007; Steele et al. 2007; Punch 2007).

Variability time-scales τ are intimately linked to the extension of the region R from which the observed emission originates by the causality condition $R \lesssim \delta c\tau/(1+z)$. Cui (2004) has suggested that the flare hierarchy seen in Mkn 501 long-term data implies a scale-invariant nature of the flare process and that there might not be any fundamental difference among long, intermediate and rapid flares. Although not thoroughly understood, the flares in blazars might be related to internal shocks in the jet (Rees 1978;

² available at <http://xte.mit.edu/>

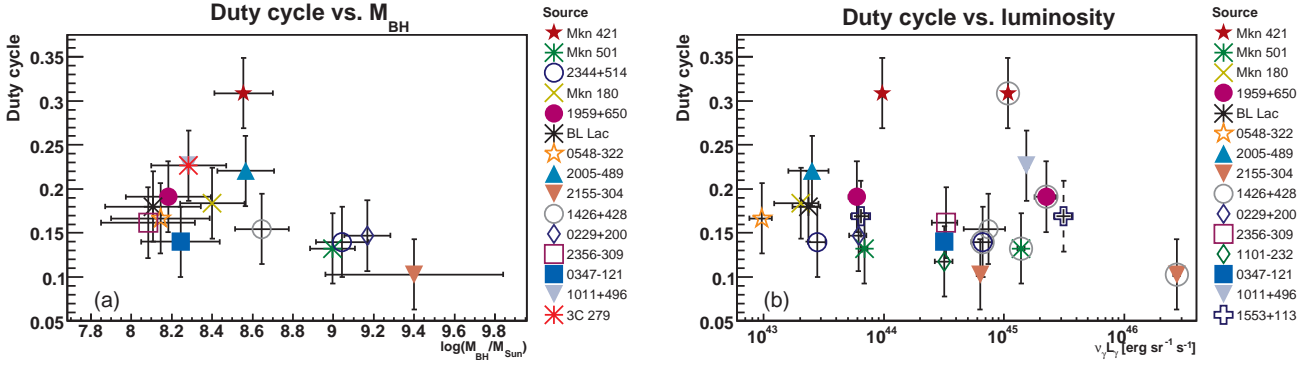


Figure 16. Correlations of the X-ray duty cycle with (a) the BH mass and (b) the VHE luminosity.

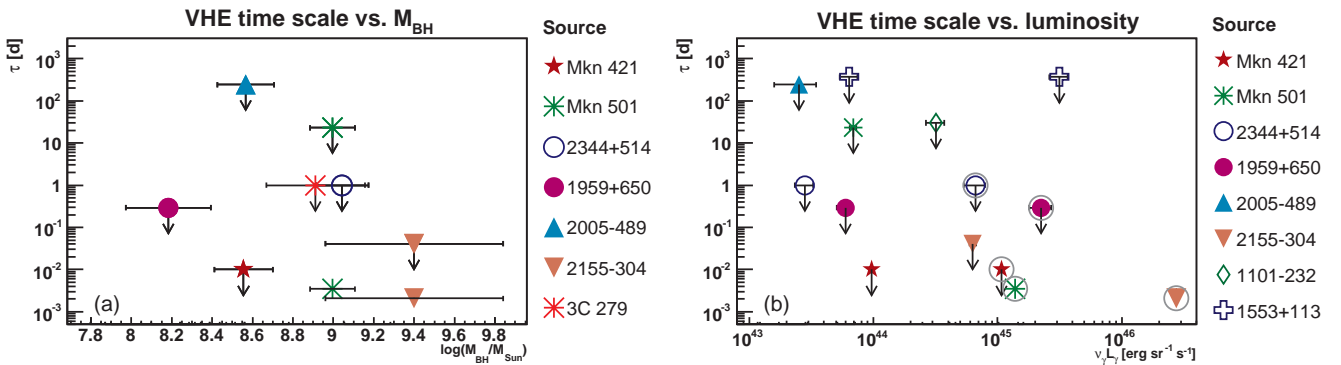


Figure 17. Correlations of the VHE γ flux doubling time τ with (a) the BH mass and (b) the VHE luminosity. Upper limits on τ are taken from Costamante et al. (2007) and from the references given in Tab. 3. Additional data points represent the recently found fast doubling times for Mkn 501 (Albert et al. 2007f) and PKS 2155-304 (Aharonian et al. 2007b). Further for Mkn 421 (Gaidos et al. 1996), IES 2344+514, and IES 1959+650 doubling times during flare states are also included, which are marked by additional grey circles. The two data points for PG 1553+113 represent assumed redshifts of $z = 0.1$ (lower luminosity) and $z = 0.3$ (higher luminosity), respectively.

Spada et al. 2001) or to major ejection events of new components of relativistic plasma into the jet (Böttcher, Maue & Schlickeiser 1997; Mastichiadis & Kirk 1997). Different flare time-scales thus may be caused by a hierarchy of inhomogeneities in the jet, energised so as to produce flares. As a timing property of the VHE γ -ray emission, we collect the minimum flux doubling times found from literature for the VHE blazars and plot them versus M_{\bullet} (Fig. 17a) and the VHE luminosity (Fig. 17b). Because of the very limited data base of VHE variability measurements, which also is biased towards high-flux states and outbursts, time-scales are mostly given as upper limits, which disables strong conclusions.

The observed VHE flux doubling times do not scale with the BH mass (Fig. 17a), which may simply mean that (1) the flaring mechanism is working in a much smaller region than the BH radius/least stable orbit and more importantly (2) the BH and its properties as such do not influence the flaring process substantially, and the embedding environment of the BH and the jet environment play more dominant roles (e.g., the accretion power of the system). The extremely short doubling times of $\tau < 5$ min recently found for Mkn 501 (Albert et al. 2007f) and PKS 2155-304 (Aharonian et al. 2007b) clearly do not support such a scaling either; even more, they are vastly incompatible with the rotation period of particles on the last stable orbit, which e.g. for the BH in Mkn 501 is $T = 8.4$ d. Additionally, the size scale implied by $\tau < 5$ min requires large Doppler factors δ in the γ -ray production regions as to avoid self-absorption. In contrast to the expected scaling behaviour of the flow

properties around BH with their masses, the three AGNs that host rather massive BHs, PKS 2155-304, Mkn 501, and Mkn 421 were found to exhibit the shortest variability time-scales. Until minute-scale flaring was found in PKS 2155-304, one could have argued that short time variability could only be measured for high fluxes due to the proximity of the respective sources: Mkn 421 and Mkn 501 are the closest blazars at $z < 0.034$, while PKS 2155-304 is located at $z = 0.116$. The present observations could, however, still be the cause of a selection effect: Minute-scale flares were found only during exceptional high-flux states of the respective sources so far. In Fig. 18 we translate the BH masses into the corresponding gravitational radii $r = GM/c^2$ ($=0.5$ Schwarzschild radius) and the observed minimal variability time-scales into the sizes of the emission regions $R \lesssim \delta c\tau/(1+z)$, assuming $\delta = 10$. For blazars in which fast variability has been observed, the extreme compactness of the emission region is apparent, being clearly comparable to or smaller than the Schwarzschild radius of the central BH. Even if the flares were driven by extremely large Doppler factors, say $\delta \approx 100$, this would still result in emission regions smaller than the Schwarzschild radius for the Mkn 501 and PKS 2155-304 flares.

6 CONCLUDING REMARKS

Before the new generation of IACT became operational, only six firmly detected extragalactic VHE γ -ray sources were known (e.g.,

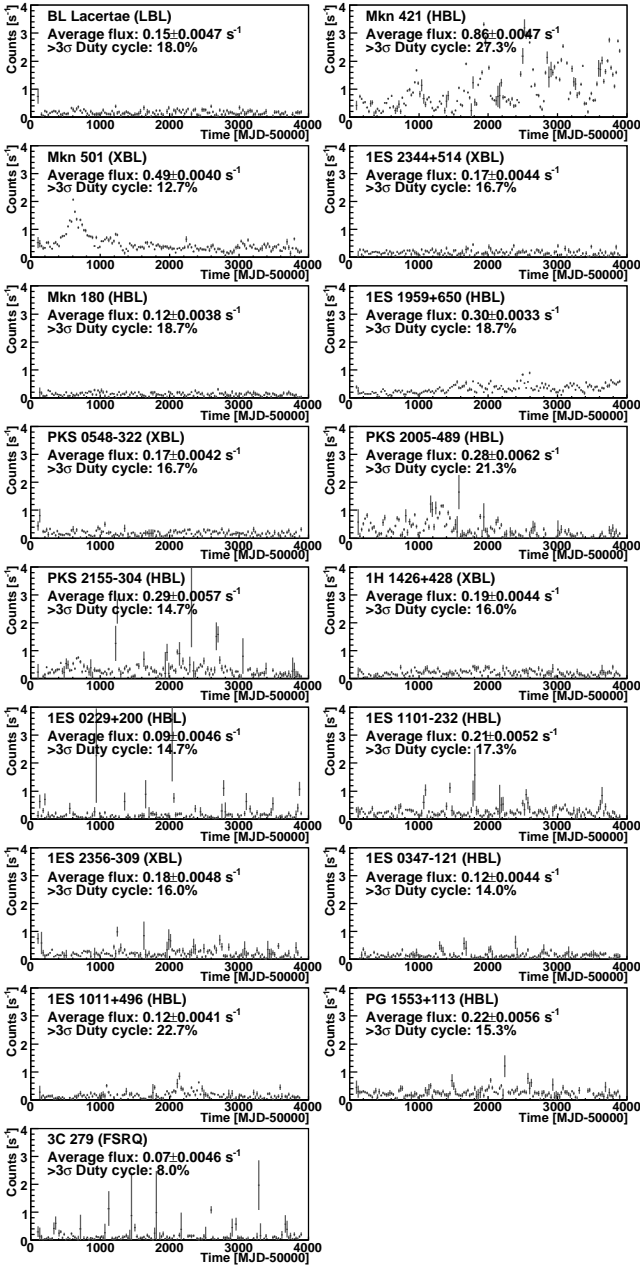


Figure 15. X-ray (2–10 keV) light curves of VHE γ -ray emitting blazars. The flare duty cycle, i.e. the fraction of time in which the respective object significantly exceeds its average X-ray flux by 50 per cent is shown. For convenience the ranges of the vertical axes are fixed for all plots. FSRQ: Flat spectrum radio quasar, LBL: low-frequency peaked BL Lac object; HBL: high-frequency peaked BL Lac object, synchrotron peak in the UV/X-ray range; XBL: extreme BL Lac object.

Mori 2003); not for all of them differential energy spectra had been inferred. To date, there are 17 BL Lac objects and the FSRQ 3C 279 known to emit VHE γ -rays. This substantially enlarged set of blazars called for a synoptic study. We collected and derived intrinsic properties of the VHE γ -ray emission (luminosity, spectral hardness, temporal properties) and further included X-ray, optical, and radio emission properties. As an accessible property of the BHs in the centres of the blazar host galaxies, the BH mass was also used. The studies yield the following results:

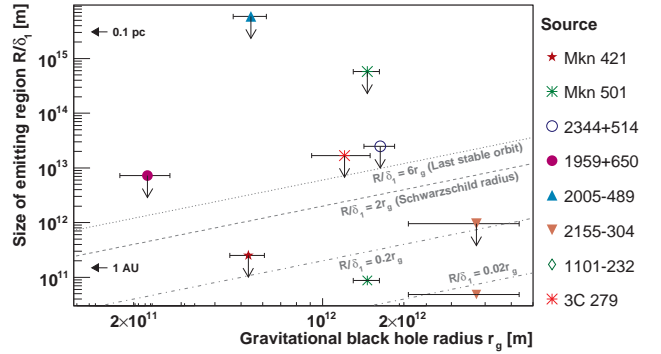


Figure 18. Gravitational radius r_g vs. upper limits on the size of the VHE γ -ray emission region R determined by the causality condition. $\delta_1 = 10 \cdot \delta$ denotes the Doppler factor. The lines correspond to emission region sizes of the last stable orbit radius (dotted line), of the Schwarzschild radius (dashed line), and of 10 per cent and 1 per cent of the Schwarzschild radius, respectively (dot-dashed line).

- So far, only blazars with $M_\bullet \gtrsim 10^8 M_\odot$ show VHE γ emission.
- The VHE luminosity of the blazars under study and the corresponding X-ray luminosity show a hint of a correlation, as expected from leptonic acceleration/SSC models.
- A correlation between the spectral slope in the VHE region and the peak location of the synchrotron peak is found. Such a correlation is also expected from SSC models.
- There are no correlations of the γ emission properties with the BH masses of the galaxies that host the blazars. Also, no correlation of the BH mass could be observed with the flare duty cycles and the flare time-scales. Thus, the BH mass itself seems not to be a dominant property for the VHE γ -ray emission. Other possibly interesting BH parameters are not yet within instrumental reach.
- There is an indication that the VHE γ luminosity is correlated with the spectral hardness. This correlation can be formulated as a decrease of $\Delta\Gamma \approx 0.82$ per decade of luminosity.
- This behaviour is also found for some individual blazars that were observed in different emission states: There are indications that in some variable sources the observed spectra become harder with increasing luminosity, while in others no hardening is found.

Investigations of the temporal properties of the X-ray emission show that the blazars with the most massive BHs have rather low duty cycles. The temporal behaviour of the VHE γ -ray emission is not well studied for most of the VHE blazars, but the present data do not seem to support a scaling of the flux doubling time-scales with the BH masses.

Obviously we are still dealing with a low number of sources and certainly with an incomplete source sample, which leaves regions in the parameter space empty. Nevertheless, the rather impressive number of 18 blazars now seen in VHE γ -rays has permitted first comparative studies. It also allows conclusions concerning EBL models: A hint at a marginal correlation between the intrinsic spectral hardness and the source distance is likely due to an EBL over-prediction. This result was also recently quantified by Aharonian et al. (2006a) using the two distant blazars 1ES 1101-232 and H 2356-309. In clarifying the situation, more distant sources particularly with intrinsically hard spectra (as e.g. 1ES 0229+200) will play a decisive role; PG 1553+113 with its yet undetermined distance might also turn out to be a good candidate for such analyses once a measurement of its redshift succeeds. In the meantime, the observed luminosity distribution of the

studied VHE γ blazars was used to constrain unknown distance of PG 1553+113 by assuming that the properties of this blazar are not too different from the most extreme objects in the blazar sample. Conversely, a large distance of PG 1553+113 implies an unusually high luminosity or an unusually high Doppler factor.

It can be said that the era of blazar astronomy has been entered – astronomy being understood as the study of generic properties of a given class of objects. With the currently known VHE blazars and the given instrumental sensitivity, VHE blazar astronomy starts to become less biased: Not only blazars with hard spectra or during outbursts have been detected, but also low (quiescent?) emission states in the VHE range are now being observed and studied.

With continuing discoveries of new sources, it will become easier to disentangle EBL absorption effects and intrinsic absorption effects from the measured spectra. Already currently, the VHE blazar sample contains groups of objects at very similar distances, e.g. 1ES 1218+304 and 1ES 1101-232 ($\Delta z = 0.004$), or the triplet 1ES 2344+514, Mkn 180, and 1ES 1959+650 ($\Delta z = 0.003$). Such groups are ideal for direct comparisons between the respective individual objects, as they are subject to very similar EBL attenuation.

Since 2003, on average three new blazars have been detected per year. When comparing this rate to the ten years it took to discover the first six VHE blazars, one can with good reason hope to accumulate many more sources in the near future, which will refine synoptic blazar studies as the pioneering one conducted here. In addition, the first observation of new object classes like LBLs and FSRQs will certainly help to sharpen the VHE view of a possible blazar sequence and the underlying physics in the near future.

ACKNOWLEDGMENTS

Luigi Costamante kindly provided the full object list from Costamante & Ghisellini (2002). I would like to thank Eckart Lorenz, Włodęk Bednarek, Nina Nowak, and Hinrich Meyer for fruitful discussions on this study and the *RXTE* team for providing the all-sky monitor X-ray data. The financial support by Max Planck Society is gratefully acknowledged.

REFERENCES

- Aharonian F. A., 2000, *NewA*, 5, 377
- Aharonian F., et al. (HEGRA collab.), 1999a, *A&A*, 342, 69
- Aharonian F. A., et al. (HEGRA collab.), 1999b, *A&A*, 350, 757
- Aharonian F. A., et al. (HEGRA collab.), 2001a, *A&A*, 366, 62
- Aharonian F. A., et al. (HEGRA collab.), 2001b, *ApJ*, 546, 898
- Aharonian F., et al. (HEGRA collab.), 2002, *A&A*, 384, L23
- Aharonian F. A., et al. (HEGRA collab.), 2004, *A&A*, 421, 529
- Aharonian F. A., et al. (H.E.S.S. collab.), 2005a, *A&A*, 430, 865
- Aharonian F. A., et al. (H.E.S.S. collab.), 2005b, *A&A*, 436, L17
- Aharonian F., et al. (H.E.S.S. collab.), 2005c, *A&A*, 441, 465
- Aharonian F. A., et al. (H.E.S.S. collab.), 2006a, *Nat*, 440, 1018
- Aharonian F. A., et al. (H.E.S.S. collab.), 2006b, *A&A*, 448, L19
- Aharonian F., et al. (H.E.S.S. collab.), 2006c, *Sci*, 314, 1425
- Aharonian F., et al. (H.E.S.S. collab.), 2007a, *A&A*, 470, 475
- Aharonian F., et al. (H.E.S.S. collab.), 2007b, *ApJ*, 664, L71
- Aharonian F., et al. (H.E.S.S. collab.), 2007c, *A&A*, 473, L25
- Albert J., et al. (MAGIC collab.), 2006a, *ApJ*, 639, 761
- Albert J., et al. (MAGIC collab.), 2006b, *ApJ*, 642, L119
- Albert J., et al. (MAGIC collab.), 2006c, *ApJ*, 648, L105
- Albert J., et al. (MAGIC collab.), 2007a, *ApJ*, 654, L119
- Albert J., et al. (MAGIC collab.), 2007b, *ApJ*, 662, 892
- Albert J., et al. (MAGIC collab.), 2007c, *ApJ*, 663, 125
- Albert J., et al. (MAGIC collab.), 2007d, *ApJ*, 666, L17
- Albert J., et al. (MAGIC collab.), 2007e, *ApJ*, 667, L21
- Albert J., et al. (MAGIC collab.), 2007f, *ApJ*, 669, 862
- Albert J., et al. (MAGIC collab.), 2007g, *ApJ*, subm., preprint: arXiv:0706.4453 [astro-ph]
- Baixeras C., et al. (MAGIC collab.), 2004, *Nucl. Instr. Meth.*, A518, 188
- Barth A. J., Ho L. C., Sargent W. L. W., 2003, *ApJ*, 583, 134
- Bednarek W., 1993, *ApJ*, 402, L29
- Benbow W., Bühler R. (H.E.S.S. collab.), 2007, in Proceedings of the 30th International Cosmic Ray Conference, Merida, preprint: arXiv:0709.4598 [astro-ph]
- Benbow W., Boisson C., Bühler R., Sol H. (H.E.S.S. collab.), 2007, in Proceedings of the 30th International Cosmic Ray Conference, Merida, preprint: arXiv:0709.4602 [astro-ph]
- Bender R., Kormendy J., 2003, in Shaver P., Dilella L., Giménez A., eds, *Astronomy, Cosmology and Fundamental Physics*, p. 262
- Bettoni D., Falomo R., Fasano G., Govoni F., Salvo M., Scarpa R., 2001, *A&A*, 380, 471
- Blandford R. D., 1976, *MNRAS*, 176, 465
- Blandford R. D., Königl A., 1979, *ApJ*, 232, 34
- Blandford R. D., Payne D. G., 1982, *MNRAS*, 199, 883
- Blandford R. D., Znajek R. L., 1977, *MNRAS*, 179, 433
- Błażejowski M., Blaylock G., Bond I. H., et al., 2005, *ApJ*, 630, 130
- Böttcher M., Mause H., Schlickeiser R., 1997, *A&A*, 324, 395
- Buckley J. H., et al. (Whipple collab.), 1996, *ApJ*, 472, L9
- Catanese M., et al. (Whipple collab.), 1998, *ApJ*, 501, 616
- Chadwick P. M., et al., 1999, *ApJ*, 513, 161
- Cogan P. (VERITAS collab.), 2007, in Proceedings of the 30th International Cosmic Ray Conference, Merida, preprint: arXiv:0709.3695 [astro-ph]
- Coppi P. S., 1992, *MNRAS*, 258, 657
- Cortina J., et al. (MAGIC collab.), 2005, in Proceedings of the 29th International Cosmic Ray Conference Vol. 5, Pune, pp 359–362
- Costamante L., Ghisellini G., 2002, *A&A*, 384, 56
- Costamante L., Ghisellini G., Giommi P., Tagliaferri G., Celotti A., Chiantera M., Fossati G., Maraschi L., Tavecchio F., Treves A., Wolter A., 2001, *A&A*, 371, 512
- Costamante L., Benbow W., Boisson C., Pita S., Sol H. (H.E.S.S. collab.), 2007, in Proceedings of the 30th International Cosmic Ray Conference, Merida, preprint in: arXiv:0710.4057 [astro-ph], p. 122
- Cui W., 2004, *ApJ*, 605, 662
- Daniel M. K., et al. (Whipple collab.), 2005, *ApJ*, 621, 181
- Dar A., Laor A., 1997, *ApJ*, 478, L5
- Denn G. R., Mutel R. L., Marscher A. P., 2000, *ApJS*, 129, 61
- Dermer C. D., Schlickeiser R., 1994, *ApJS*, 90, 945
- Djorgovski S., Davis M., 1987, *ApJ*, 313, 59
- Donato D., Ghisellini G., Tagliaferri G., Fossati G., 2001, *A&A*, 375, 739
- Edwards P. G., Piner B. G., 2002, *ApJ*, 579, L67
- Falomo R., 1996, *MNRAS*, 283, 241
- Falomo R., Kotilainen J. K., Treves A., 2002, *ApJ*, 569, L35
- Falomo R., Scarpa R., Bersanelli M., 1994, *ApJS*, 93, 125
- Falomo R., Treves A., 1990, *PASP*, 102, 1120
- Ferrarese L., Merritt D., 2000, *ApJ*, 539, L9
- Fossati G., Maraschi L., Celotti A., Comastri A., Ghisellini G., 1998, *MNRAS*, 299, 433
- Gaidos J. A., et al. (Whipple collab.), 1996, *Nature*, 383, 319

- Gebhardt K., Bender R., Bower G., Dressler A., Faber S. M., et al., 2000, *ApJ*, 539, L13
- Goebel F., Backes M., Wagner R. M., Bretz T., Hayashida M., Hsu C.-C., Mannheim K., Mazin D., 2007, in *Proceedings of the 30th International Cosmic Ray Conference*, Merida, preprint: arXiv:0709.2032 [astro-ph]
- Gould R. J., Schröder G., 1966, *PRL*, 16, 252
- Graham A. W., 2007, *MNRAS*, 379, 711
- Gu M., Cao X., Jiang D. R., 2001, *MNRAS*, 327, 1111
- Hartman R. C., Bertsch D. L., Bloom S. D., et al., 1999, *ApJS*, 123, 79
- Hauser G. H., Dwek E., 2001, *ARA&A*, 39, 249
- Hinton J., 2004, *NewAR*, 48, 331
- Hogg D. W., Baldry I. K., Blanton M. R., Eisenstein D. J., 2002, preprint: astro-ph/0210394
- Horan D., Finley J. P., 2001, in *Proceedings of the 27th International Cosmic Ray Conference*, Hamburg, p. 2622
- Horan D., et al. (Whipple collab.), 2002, *ApJ*, 571, 753
- Horan D., et al. (Whipple collab.), 2004, *ApJ*, 603, 51
- Jester S., Harris D. E., Marshall H. L., Meisenheimer K., 2006, *ApJ*, 648, 900
- Kashlinsky A., 2005, *Phys. Rep.*, 409, 361
- Katarzyński K., Ghisellini G., Tavecchio F., Gracia J., Maraschi L., 2006a, *MNRAS*, 368, L52
- Katarzyński K., Ghisellini G., Mastichiadis A., Tavecchio F., Maraschi L., 2006b, *A&A*, 453, 47
- Kerrick A. D., et al. (Whipple collab.), 1995, *ApJ*, 452, 588
- Kneiske T. M., Bretz T., Mannheim K., Hartmann D. H., 2004, *A&A*, 413, 807
- Kormendy J., Richstone D., 1995, *ARA&A*, 33, 581
- Krawczynski H., et al., 2001, *ApJ*, 559, 187
- Krawczynski H., et al., 2004, *ApJ*, 601, 151
- Krennrich F., et al. (Whipple collab.), 2001, *ApJ*, 560, L45
- Krennrich F., et al. (Whipple collab.), 2002, *ApJ*, 575, L9
- Kudoh T., Aoki S., Koide S., Shibata K., 1999, *Astron. Nachr.*, 320, 311
- Liu Y., Jiang D. R., Gu M. F., 2006, *ApJ*, 637, 669
- Lynden-Bell D., 1969, *Nature*, 223, 690
- Malkov M. A., Drury L. O., 2001, *Rep. Prog. Phys.*, 64, 429
- Mannheim K., 1993, *A&A*, 269, 67
- Maraschi L., et al., 1999, *ApJ*, 526, L81
- Maraschi L., Ghisellini G., Celotti A., 1992, *ApJ*, 397, L5
- Mastichiadis A., Kirk J. G., 1997, *A&A*, 320, 19
- Mazin D., 2003, *Diplomarbeit*, Universität Hamburg
- Mazin D., Goebel F., 2007, *ApJ*, 655, L13
- McHardy I. M., Koerding E., Knigge C., Uttley P., Fender R. P., 2006, *Nat*, 444, 730
- McLure R. J., Dunlop J. S., 2002, *MNRAS*, 331, 795
- Miller H. R., Green R. F., 1983, *BAAS*, 15, 957
- Mirabel I. F., 2004, in *Schönfelder V., Lichti G., Winkler C., eds, ESA SP-552: 5th INTEGRAL Workshop on the INTEGRAL Universe*, p. 175
- Mirabel I. F., Rodríguez L. F., 1999, *ARA&A*, 37, 409
- Mori M., 2003, in *Proceedings of the 28th International Cosmic Ray Conference*, Vol. 8. Tsukuba, p. 161
- Mücke A., Protheroe R. J., 2001, *APh*, 15, 121
- Nieppola E., Tornikoski M., Valtaoja E., 2006, *A&A*, 445, 441
- Nikishov A. I., 1962, *Sov. Phys. JETP*, 14, 393
- Nishijima K., 2002, *PASA*, 19, 26
- Nishiyama T., et al. (Utah Seven Telescope Array collab.), 1999, in *Proceedings of the 26th International Cosmic Ray Conference Vol. 3*, Salt Lake City, p. 370
- Piner B. G., Edwards P. G., 2004, *ApJ*, 600, 115
- Piner B. G., Unwin S. C., Wehrle A. E., Edwards P. G., Fey A. L., Kingham K. A., 1999, *ApJ*, 525, 176
- Piner B. G., Pant N., Edwards P. G., 2007, in *Rector T. A., De Young D. S., eds, in Proceedings of Extragalactic Jets – Theory and Observation from Radio to Gamma Ray*, Girdwood, ASP Conf. Ser., in press
- Primack J. R., Bullock J. S., Somerville R. S., 2005, in *Aharonian F. A., Völk H. J., Horns D., eds, High Energy Gamma-Ray Astronomy*, AIP Conf. Ser. 745, pp 23–33
- Punch M. (H.E.S.S. collab.), 2007, in *Proceedings of the 30th International Cosmic Ray Conference*, Merida, preprint in: arXiv:0710.4057 [astro-ph], p. 106
- Punch M., et al. (Whipple collab.), 1992, *Nat*, 358, 477
- Quinn J., et al. (Whipple collab.), 1996, *ApJ*, 456, L83
- Raue M., Benbow W., Costamante L., Horns D. (H.E.S.S. collab.), 2007, in *Proceedings of the 30th International Cosmic Ray Conference*, Merida, preprint in: arXiv:0710.4057 [astro-ph], p. 134
- Rebillot P. F., Badran H. M., Blaylock G., et al., 2006, *ApJ*, 641, 740
- Rees M. J., 1978, *Nat*, 275, 516
- Rees M. J., 1978, *ARA&A*, 184, 61P
- Richstone D., et al., 1998, *Nat*, 395, A14
- Sbarufatti B., Treves A., Falomo R., Heidt J., Kotilainen J., Scarpa R., 2006, *AJ*, 132, 1
- Schroedter M., et al. (Whipple collab.), 2005, *ApJ*, 634, 947
- Sikora M., Begelman M. C., Rees M. J., 1994, *ApJ*, 421, 153
- Spada M., Ghisellini G., Lazzati D., Celotti A., 2001, *MNRAS*, 325, 1559
- Spergel D. N., et al., 2007, *ApJS*, 170, 377
- Stecker F. W., Malkan M. A., Scully S. T., 2006, *ApJ*, 648, 774
- Steele D. (VERITAS collab.), Carini M. T., Charlot P., Kurtanidze O., Lahteenmaki A., Montaruli T., Sadun A. C., Villata M., 2007, in *Proceedings of the 30th International Cosmic Ray Conference*, Merida, preprint: arXiv:0709.3869 [astro-ph]
- Superina G., Benbow W., Boutelier T., Dubus G., Giebels B. (H.E.S.S. collab.), 2007, in *Proceedings of the 30th International Cosmic Ray Conference*, Merida, preprint in: arXiv:0710.4057 [astro-ph], p. 138
- Tavecchio F., Maraschi L., Ghisellini G., 1998, *ApJ*, 509, 608
- Teshima M., et al. (MAGIC collab.), 2007, in *Proceedings of the 30th International Cosmic Ray Conference*, Merida, preprint: arXiv:0709.1475 [astro-ph]
- Thuczykont M., Shayduk M., Kalekin O., Bernardini E., 2007, *J. Phys. Conf. Ser.*, 60, 318
- Tremaine S., et al., 2002, *ApJ*, 574, 740
- Treves A., Falomo R., Uslenghi M., 2007, *A&A*, accepted, preprint: arXiv:0709.1271 [astro-ph]
- Uchiyama Y., Urry C. M., Cheung C. C., Jester S., van Duyne J., Coppi P., Sambruna R. M., Takahashi T., Tavecchio F., Maraschi L., 2006, *ApJ*, 648, 910
- Urry C. M., Padovani P., 1995, *PASP*, 107, 803
- Venters T. M., Pavlidou V., 2007, *ApJ*, 666, 128
- Wagner R. M., Dorner D., Goebel F., Hengstebeck T., Kranich D., Mazin D., Tesaro D. (MAGIC collab.), Nowak N., 2007, in *Proceedings of the 30th International Cosmic Ray Conference*, Merida, preprint: arXiv:0711.1586 [astro-ph]
- Woo J.-H., Urry C. M., 2002a, *ApJ*, 579, 530
- Woo J.-H., Urry C. M., 2002b, *ApJ*, 581, L5
- Woo J.-H., Urry C. M., van der Marel R. P., Lira P., Maza J., 2005, *ApJ*, 631, 762
- Wu X.-B., Liu F. K., Zhang T. Z., 2002, *A&A*, 389, 742